Ab Initio Modeling of Metal Adhesion on Oxide Surfaces with Defects

Yu. F. Zhukovskii,[1,2] E. A. Kotomin,[1,3] P. W. M. Jacobs,[2,*] and A. M. Stoneham[4]

[1]*Institute of Solid State Physics, University of Latvia, Kengaraga 8, LV-1063 Riga, Latvia*
[2]*Department of Chemistry, University of Western Ontario, London, Ontario, Canada N6A 5B7*
[3]*Fachbereich Physik, Universität Osnabrück, Barbarastrasse 7, D-49069 Osnabrück, Germany*
[4]*Center for Materials Research, Department of Physics and Astronomy, University College London, Gower Street, London WC1E 6BT, United Kingdom*
(Received 30 June 1999)

Our *ab initio* studies show that surface defects cause redistribution of the electron density which can increase substantially the binding energy of metal atoms to oxide surfaces. The results for electron (F_s^0) and hole (V_s^0) centers in the adhesion of Ag atoms (at 1:4 and 1:1 coverages) to a MgO(100) surface, combined with previous studies for charged defects, support earlier ideas of the mechanism of radiation-enhanced adhesion of nonreactive metals on oxide substrates. The results suggest that some optical control of adhesion energies is possible through charge transfer.

PACS numbers: 68.35.–p, 71.15.–m

Given that metal-oxide interfaces are critical to many areas of technology (e.g., [1–3]), from protective oxides through nuclear fuel-clad interactions to catalysis, the control of interfacial energies has special importance. Here, we extend ideas proposed earlier on the basis of the image interaction model [4] which suggest a key role for defects, especially charged defects. Our *ab initio* studies show that these basic ideas were largely correct. The relation between interface strength and its atomic/electronic structure is a complex one [5,6], and open questions remain, despite many studies of the adhesion of noble and transition metals to metal oxides. In our calculations [7] on the slab model of a perfect Ag/MgO(100) interface, we used the Hartree-Fock (HF) method with electron correlation corrections [8] as implemented in the CRYSTAL95 computer code [9]. Generalizing these large-scale calculations to complex technological situations demands much simpler methods, such as the phenomenological atomistic shell model (SM) [10] and image interaction model (IIM) [4]. One of the implications of the IIM was that charged defects could give rise to significant changes in interfacial energies [4], and it is this idea we extend in the present Letter.

In our new calculations on the Ag/MgO(100) interface with defects, we again used the *ab initio* HF computer code CRYSTAL95 for periodic systems [9] with Perdew-Wang generalized gradient approximation *a posteriori* electron correlation corrections to the total energy [11]. The basis sets (BSs) used were all-electron 8-61G for Mg and 8-51G for O. For Ag we used a small core Hay-Wadt pseudopotential with a 311-31G BS for the $4s^2 4p^6 4d^{10} 5s^1$ electrons. We simulated the Ag/MgO(100) interface as a slab with either a low (1:4) surface coverage by Ag atoms, which models the initial stage of metal film adhesion [Figs. 1(a) and 1(b)], or as one to three Ag layers atop three layers of the oxide substrate. Surface defects on the MgO(100) substrate were modeled by removing one of four O or Mg atoms from the 2×2 extended surface unit cell [Figs. 1(c) and 1(d)], leaving in the vacancy the BS of the missing atom (the so-called *ghost* [9]), thus creating electron F_s or hole V_s centers. The atomic relaxation of the substrate structure around these defects was found first for MgO slabs and then reoptimized for the Ag/MgO interfaces with defects. Results summarized in Table I show the effects of defect density, though not negligible, are generally small and unlikely to have a dominant influence.

Table II summarizes our main results. For full Ag (1:1) coverage, adsorption over the O atoms on the *perfect* MgO surface is the most favorable energetically. This agrees with both recent experiments [14] and previous local-density-approximation–type calculations [2]. For the favored Ag configuration over O, the equilibrium interface distances calculated by all the microscopic methods lie within the range 2.4 to 2.7 Å; the image model result also agrees, giving 2.53 Å [12]. Our value of 2.43 Å for three metal layers coincides with recent experimental data [14]. As the number of Ag(100) planes changes from one to three, the adhesion energy over regular O atoms increases from 0.25 eV up to 0.46 eV, but it has little effect on silver adhesion over a Mg atom. Experimentally, the relevant Ag adhesion energy is estimated as 0.26 eV [15], presumably lower than the value for a perfect surface because of misfit dislocations due to the 3% difference in lattice parameters of Ag and MgO crystals, neglected in our calculations.

The calculated Mulliken charges on Ag atoms ($\Delta q^{(Ag)}$ in Table II) indicate negligible charge transfer between MgO and Ag, in agreement with IIM calculations [16]. The bond populations across the interface [between Ag atoms and ions of the perfect MgO(100) substrate] are also practically zero. The dominant effects are *physical adhesion* associated with Ag polarization and charge redistribution. Adhesion energy is enhanced by interaction of substrate ions with the extra electron density near hollow positions of the interfacial Ag layer. This favors Ag atoms placed above surface O^{2-} ions, as observed experimentally [17].
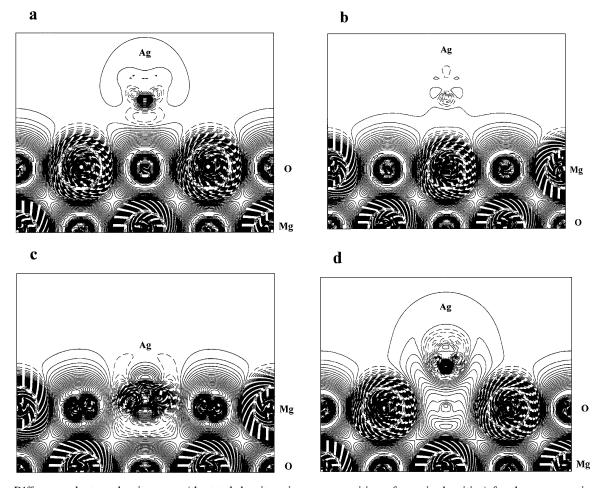
FIG. 1.   *Difference* electron density maps (the total density minus superposition of atomic densities) for the cross section perpendicular to the (100) interface plane for 1:4 Ag adsorption (a) over a regular O^{2-} surface ion, (b) over a regular Mg^{2+} surface ion, (c) over the surface V_s^0 center, and (d) over the surface F_s^0 center. Isodensity curves are drawn from $-0.8e\,a_0^{-3}$ to $+0.8e\,a_0^{-3}$ with an increment of $0.002e\,a_0^{-3}$. The full, dashed, and chained curves show positive, negative, and zero difference electron densities, respectively. Note that Ag atoms are strongly polarized: Above O^{2-} ions (a), the electron density is shifted in the direction outwards from the surface, whereas, above magnesium (b), it is shifted towards surface Mg^{2+}. The Ag^{2+} ion substituting for an Mg^{2+} ion (c) is visibly deformed, and there is noticeable bonding in the Ag^{-}-F_s^{+} complex (d) but electron density is considerably delocalized from the vacancy.

It is this small but significant charge, plus differences in dispersion forces, which are the main reasons for differences in predictions of the IIM model and our HF slab simulations. The atomic dipole moments $D_z^{(Ag)}$ (Table II) characterize a shift of electron density along the z axis (the outward normal to the surface [9]). As expected from the IIM, $D_z^{(Ag)}$ has opposite signs above O and above Mg (except for the three-layer silver film), corresponding to electrons being repelled by the anion or attracted by the cation. For the Ag monolayer, $D_z^{(Ag)}$ is largest for Ag over the O sites. The component $Q_{z^2-(x^2+y^2)/2}^{(Ag)}$ of the quadrupole moment (Table II) is affected significantly by Ag 4d-5s orbital mixing. Negative values (as found in all cases except the $\frac{1}{4}$ layer) mean that the Ag atom has contracted axially in the z direction and expanded in the xy plane. For all adsorption positions $|Q_{z^2-(x^2+y^2)/2}^{(Ag)}|$ is larger than the corresponding magnitudes for surface Mg^{2+} and O^{2-}

ions by a factor of at least 4. Thus, Ag atoms adsorbed on MgO(100) surfaces are considerably deformed.

Difference electron charge distributions for 1:4 Ag coverage over O^{2-} and Mg^{2+} ions [Figs. 1(a) and 1(b)] show that silver atoms are more strongly polarized above surface O^{2-} ions. Nevertheless, magnitudes of the corresponding binding energies are close (Table II), unlike the adhesion of one and three Ag layers. This may be explained by a partial compensation of electrostatic attraction and repulsion between slightly charged silver adatoms and nearest substrate ions. Both SM [10] and HF cluster [13(b)] calculations also predict preferential adsorption over O^{2-}, but with different adhesion energies (Table II). The smaller SM value may result from the neglect of the electron density redistribution within the metal film.

In calculations for a *defective* MgO surface, we first optimized the geometry of a pure MgO(100) slab around neutral F_s^0 and V_s^0 centers. When a ghost orbital is centered

TABLE I.   Effect of supercell size on valence- and defect-band parameters.

| Model of MgO(100) | Valence band (eV) | | | Defect band (eV) | | | Defect |
surface	bottom	top	width	bottom	top	width	charge (e)
Perfect, 2×2 unit cell	-14.10	-9.25	4.84	$\cdots$	$\cdots$	$\cdots$	$\cdots$
F_s center, 2×2 unit cell	-13.71	-8.95	4.76	-2.577	-1.472	1.105	1.713
Perfect, 3×3 unit cell	-13.65	-9.25	4.40	$\cdots$	$\cdots$	$\cdots$	$\cdots$
F_s center, 3×3 unit cell	-13.50	-9.14	4.40	-2.155	-2.003	0.152	1.708

inside the oxygen vacancy [9], its population of $1.72e$ is typical of F^0 centers in the bulk ionic oxide; the other $0.28e$ is distributed over the two nearest spheres of ions. As a result, the F^0 center mimics the O^{2-} ion it replaces, and its energy level lies 4.2 eV above the top of the valence band. If we neglect ghost orbitals, the oxygen vacancy becomes doubly charged and the two electrons are now distributed over nearest-neighbor ions. As a result, the four surface Mg^{2+} ions are repelled from the vacancy and shift outwards by 0.16 Å; the subsurface Mg^{2+} ion is displaced into the bulk by 0.23 Å. For the V_s^0 center, the effect of ghost orbitals is small, since electron density will not be localized within the Mg^{2+} vacancy. The O^{2-} ions surrounding a Mg^{2+} vacancy shift outwards from the vacancy: Four equivalent surface O^{2-} ions move by 0.12 Å, whereas the subsurface O^{2-} ion moves toward the bulk by 0.16 Å. The four surface O^{2-} ions share 1.8 of the

V_s^0 center's two holes. These results correlate well with recent HF cluster simulations on the corresponding defective pure MgO surface [13(a)].

In calculations with Ag present (Table II), we reoptimize atomic relaxations for each position of an adsorbed Ag atom over the vacancies at which ghost orbitals are centered. When an Ag atom approaches the V_s^0 center, it donates two valence electrons to the four O^{2-} ions surrounding the Mg vacancy. These fill the two holes localized on the O^- ions of the free V_s^0 center, returning these four O^{2-} ions to the effective charges for a perfect MgO surface. ($\Delta q^{(Ag)}$ in Table II is smaller than $+2e$ by $0.5e$ due to partial electron delocalization and weak bonding with these O^{2-} ions.) This Ag^{2+} ion sits only 0.31 Å above the surface plane, and so nearly substituting for the Mg^{2+} host ion removed [Fig. 1(c)]. The large dipole and quadrupole moments and the difference electron

TABLE II.   Optimized parameters for the pure (A) and defective (B) Ag/MgO(100) interface.

Ag over	Coverage and model	Distance $l^{(0)}$(Å)	Binding energy E_b(eV)	Charge[a] $\Delta q^{(Ag)}(e)$	Dipole[b] $D_z^{(Ag)}(e\,a_0)$	Quadrupole[b] $Q_{z^2-(x^2+y^2)/2}^{(Ag)}(e\,a_0^2)$
			A. perfect interface			
	$\frac{1}{4}$ layer	2.58	0.23	0.063	0.251	-0.433
	monolayer	2.56	0.26	0.037	0.198	-2.232
Regular	3 layers	2.43	0.46	0.053^c	0.418^c	-1.971^c
O^{2-} ion	SM[d]	2.60	0.11	$\cdots$	$\cdots$	$\cdots$
	IIM[e]	2.53	0.30	$\cdots$	$\cdots$	$\cdots$
	cluster[f]	2.52	0.58	$\cdots$	$\cdots$	$\cdots$
	$\frac{1}{4}$ layer	2.89	0.22	0.038	-0.170	0.414
	monolayer	3.23	0.06	0.027	-0.071	-1.288
Regular	3 layers	3.23	0.07	0.042^c	0.116^c	-0.686^c
Mg^{2+} ion	SM[d]	3.20	0.02	$\cdots$	$\cdots$	$\cdots$
	IIM[e]	2.74	0.60	$\cdots$	$\cdots$	$\cdots$
	cluster[f]	3.95	0.01	$\cdots$	$\cdots$	$\cdots$
			B. defective interface			
F_s center	$\frac{1}{4}$ layer	1.83^g	7.59	$0.95\,(0.92)^h$	$-1.61\,(-0.71)^h$	$4.17\,(0.26)^h$
	cluster[f]	2.15^g	0.99	0.58	$\cdots$	$\cdots$
V_s center	$\frac{1}{4}$ layer	0.31^g	12.67	$-1.46\,(0.09)^h$	$0.74\,(0.16)^h$	$0.45\,(0.2)^h$
	cluster[f]	0.39^g	11.97	-1.53	$\cdots$	$\cdots$

[a]Positive sign means an excess of electron density compared to a neutral Ag atom.
[b]The values of dipole and quadrupole moments are given in atomic units ($1a_0 = 1$ bohr).
[c]For the interfacial silver layer.
[d]The shell model calculations [10] for 10 Ag layers atop 31 MgO planes.
[e]The image interaction model [12].
[f]Cluster HF calculations [13(b)].
[g]The distance between the Ag ion and the center of the vacancy.
[h]Charges and multipole moments of ghost functions centered on vacancies are given in parentheses.

density maps indicate that the Ag^{2+} ion is quite strongly polarized and deformed (cf. similar data for Ag atom adsorption on the perfect surface in Table II). The binding energy is very high, 12.67 eV, and stems from a very large electrostatic stabilization effect.

For Ag atom adsorption over F_s^0 centers, we find the opposite effect: One electron is transferred *from* the surface defect *to* the Ag atom, again yielding a pair of oppositely charged defects, Ag^-/F_s^+ [Fig. 1(d)]. Their separation, 1.83 Å, is much smaller than for an Ag atom above O^{2-} on a regular surface. The population of the Ag^--F_s^+ bond is $0.5e$, much larger than that in the negligible bonds between all other atoms. The optimized lattice relaxation includes 0.06 Å outward in-plane displacements of Mg^{2+} from the F_s center, and 0.08 Å vertical displacement of the Mg^{2+} in the plane below the F_s center. The considerable binding energy of 7.59 eV again appears to be mainly an electrostatic interaction between Ag^- and its nearest surface ions. The large dipole and quadrupole moments in Table II show that Ag^- is strongly deformed. These results complement earlier IIM studies [16] which give the interaction energy between the doubly charged vacancy (preferentially in the subsurface plane) and a *neutral* Ag atom to be ≈ 2 eV. The latter estimate is close to the SM prediction of 2.54 eV [10] in which the effect of charge transfer to metal atoms from defects was also neglected.

Lastly, we performed calculations for the Ag *monolayer* over an array of the F_s^0 centers in the same concentration (1:4). The binding energy per 2×2 extended unit cell increases by 0.75 eV, i.e., there is an additive effect in the interaction of four Ag atoms with the defect and three regular O^{2-} ions. The adhesion energy for each of the three Ag atoms is $0.75/3 = 0.25$ eV, which is very close to that for a perfect surface. The quadrupole moments of Ag atoms (Table II) imply large deformation. It seems likely that such a monolayer would be unstable with respect to faceting.

In summary, we have shown that chemical bond formation is not important for the perfect Ag/MgO(100) interface. However, even neutral surface defects could play a crucial role in metal adsorption kinetics on oxide surfaces and in the adhesion energy of metals to oxides. This, together with previous work showing the role of charged defects, is supported by experimental studies of radiation-enhanced adhesion [1,18]. An Ag atom above a V_s^0 center donates two valence electrons to the four O atoms surrounding the Mg vacancy, becoming an Ag^{2+} ion, which is drawn towards the surface and, in effect, substitutes for the missing Mg^{2+} ion. There is a very large electrostatic stabilization effect confirmed by results of previous HF cluster simulations on adhesion of Ag, Pd, Rb [13(b)], and Cu [19] on MgO(100). In contrast, Ag atoms atop the F_s^0 centers attract one of the defect electrons, yielding a strongly bound complex Ag^-/F_s^+ of oppositely charged defects. Here, unlike Ag on the

perfect surfaces, there is considerable covalent bonding, localizing an additional $0.5e$. This charge-transfer effect was not observed in cluster calculations [13(b)]. Another important result of our work is the validation of earlier ideas [4,16] that interface defects (e.g., radiation-induced) can strongly enhance metal adhesion.

---

*Corresponding author.
Email address: pjacobs@uwo.ca
Fax number: (519) 661 3022.

[1] V. E. Heinrich and P. A. Cox, *The Surface Science of Metal Oxides* (Cambridge University Press, Cambridge, England, 1994).

[2] M. W. Finnis, J. Phys. Condens. Matter **8**, 5811 (1996).

[3] C. T. Campbell, Surf. Sci. Rep. **27**, 1 (1997); G. Renaud, Surf. Sci. Rep. **32**, 1 (1998).

[4] A. M. Stoneham and P. W. Tasker, J. Phys. C **18**, L543 (1985).

[5] C. Verdozzi, D. R. Jennison, P. A. Schultz, and M. P. Sears, Phys. Rev. Lett. **82**, 799 (1999).

[6] I. G. Batyrev, A. Alavi, M. W. Finnis, and T. Deutsch, Phys. Rev. Lett. **82**, 1510 (1999).

[7] E. Heifets, Yu. F. Zhukovskii, E. A. Kotomin, and M. Causà, Chem. Phys. Lett. **283**, 395 (1998).

[8] M. Causà and A. Zupan, Chem. Phys. Lett. **220**, 145 (1994).

[9] R. Dovesi, V. R. Saunders, C. Roetti, M. Causà, N. M. Harrison, R. Orlando, and E. Aprá, CRYSTAL-95 *User Manual* (University of Turin, Turin, 1996).

[10] J. Purton, S. C. Parker, and D. W. Bullett, J. Phys. Condens. Matter **9**, 5709 (1997).

[11] J. P. Perdew and Y. Wang, Phys. Rev. B **45**, 13 244 (1992).

[12] D. M. Duffy, J. H. Harding, and A. M. Stoneham, J. Appl. Phys. **76**, 2791 (1994).

[13] A. M. Ferrari and G. Pacchioni, (a) J. Phys. Chem. **99**, 17 010 (1995); (b) **100**, 9032 (1996).

[14] P. Guenard, G. Renaud, and B. Villette, Physica (Amsterdam) **221B**, 205 (1996).

[15] A. Trampert, F. Ernst, C. P. Flynn, H. F. Fischmeister, and M. Rühle, Acta Metall. Mater. **40**, S227 (1992).

[16] D. M. Duffy, J. H. Harding, and A. M. Stoneham, Acta Metall. Mater. **43**, 1559 (1995).

[17] M.-H. Schaffner, F. Patthey, and W.-D. Schneider, Surf. Sci. **417**, 159 (1998).

[18] J.-W. He and P. J. Møller, Chem. Phys. Lett. **129**, 13 (1986); I. Astrup and P. J. Møller, Appl. Surf. Sci. **33/34**, 143 (1988).

[19] N. C. Bacalis and A. B. Kunz, Phys. Rev. B **32**, 4857 (1985).